Tidal response shaped by nonlinear topographic control

Emil V. Stanev and Jörg-Olaf Wolff

Institute for Chemistry and Biology of the Sea (ICBM), University of Oldenburg, Germany

Abstract: We demonstrate here that the the responce of tidal basins to external forcing is largely dependent on the topographic control, the latter is effectuated through: (1) the bottom slope in the areas prone to drying and flooding, and (2) the variations in section areas of inlets and deep channels. Both controls are nonlinear and result in asymmetric (in time and space) response. The underlying physics of this signal modulation from a more or less harmonic forcing at the open sea boundary is the major focus in this study. The possible consequences for morphodynamics are also addressed focusing on some common ("universal") topographic features in seven tidal basins.

1 Introduction

The principal difference between dynamical balances in the flat near-coastal zones and the ones in the deep tidal bays is associated with the Stokes drift which becomes important if tidal range is comparable with the depth. Under such conditions the current velocity produces a larger (landward) volume transport near high water, whereas the transport near low water is smaller due to the smaller cross sectional area of the inlet (Dyer 1988). The quantification of these asymmetric transports is focal to this paper.

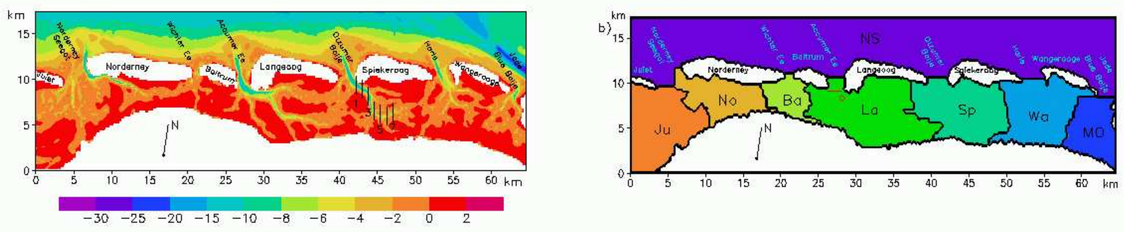

Fig. 1: Topography of the East Frisian Wadden Sea (a) and individual basins (b). The thin meridional lines in the extension of Otzumer Balje in the tidal basin of Spiekeroog Island are sections sampled every 5 minutes from the model simulations. The first section line gives also the position where ADCP observations are carried out.

2 Theory

When the basin area increases with increasing the sea-level, equal transports through the inlets produce different changes of sea-level. At low water level the changes are larger than at high water level (Fig. 2b). This means that ebb conditions evolve faster than flood conditions. The opposing effect of cross-sectional area is qualitatively illustrated in Fig. 2c.

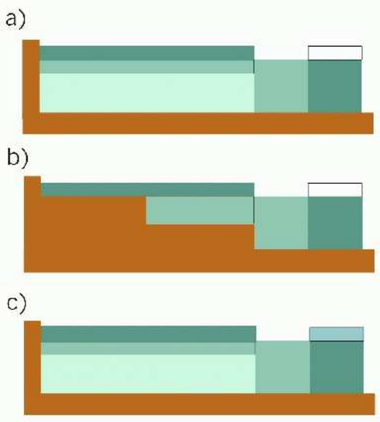

Fig. 2: Schematic representation of the bay-inlet system. (a) The bay has vertical side walls, (b) the area of the bay is a linear function of depth (Maas 1997), (c) the same as (a), but the height of water parcel is a function of the sea-level height. This case illustrates the effect of variable cross-sectional area of inlets. The difference between (c) and (a) is that the volume of water parcels entering the bay changes as a function of sea-level height. Thus the increase of sea level in the bay caused by the second water parcel in (c) is larger than the one caused by the second parcel in (a). Obviously, this effect is in opposition to the one due to hypsometry (b).

If we suppose that the forcing signal is almost harmonic $\zeta = a \sin \omega t$ with frequency ω (e. g. the semi diurnal lunar tide M_2) we can compute the tidal response as expressed by the velocity (Fig. 3).

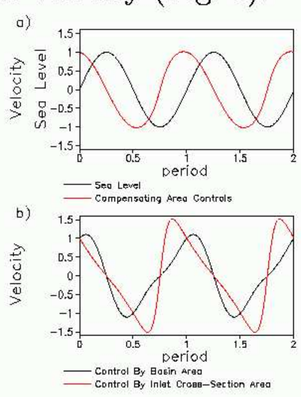

Fig. 3: Temporal asymmetries of the tidal response. (a) sea level and inlet current in the case of compensation of hypsometric and cross-section area controls, (b) currents in the case of hypsometric control (black curve) and control by the section area of inlet (red curve). Under hypsometric control it takes a longer time for the transition between maximum ebb current to maximum flood current than in the remaining part of the tidal period. The situation reverses under control of cross-section area. The results are shown in non-dimensional form. Positive values mean inward current.

3 Observations

Tidal basins undergo morphodynamic evolution triggered by the asymmetry of the response to oscillations in the open ocean. Many attempts in coastal engineering have been done to quantify the relationship between geometry of tidal basins (e. g. the tidal prism) and the cross sectional area of the inlets (O'Brien, 1936). The nonlinear topographic control caused by the linearly increasing basin area (Fig. 4) is a candidate to explain the nonlinear correlation between the observed tidal prism and cross sectional areas of the inlets for a wide spectrum of similar tidal basins.

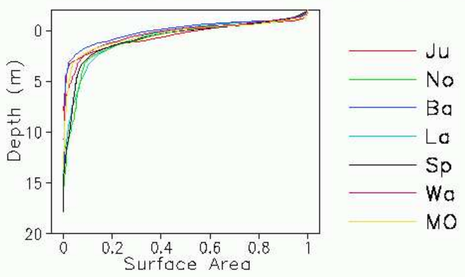

Fig. 4: Normalized hypsometric curves in the tidal basins. For the notations see Fig. 1.

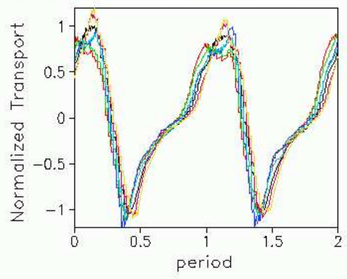

Fig. 5: Normalized transports through inlets. During most of the tidal cycle these curves lie in a tight envelope showing the universal topographic control on dynamics in the different basins. Modification of the topography could occur under extreme conditions.

The observations carried out with ADCP along section line 1 (see Fig. 1) support the theoretical estimates about the temporal asymmetries. The higher mode oscillations reveal the nonlinear response.

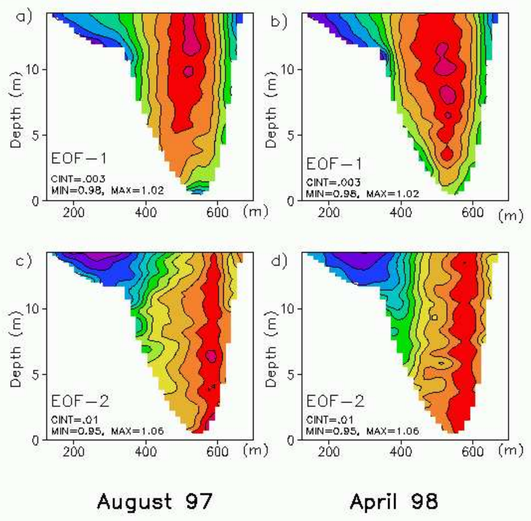

Fig. 6: The first (a) and (b) and second (c) and (d) EOF corresponding to spring (left plots) and neap (plots on the right) conditions. The analysis is done for locations below 14.5m

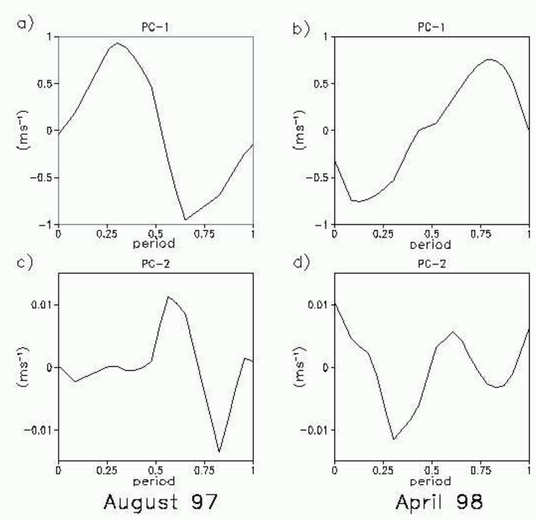

Fig. 7: The first (a) and (b) and second (c) and (d) PC corresponding to spring (left plots) and neap (plots on the right) conditions. Positive values correspond to land ward currents.

4 Numerical simulations

The General Estuarine Transport Model (Burchard and Bolding, 2000) with a horizontal resolution of 200 m is used (see for more details Stanev et al., 2003a,b). The subgrid parameterizations are based on the $k-\epsilon$ turbulent closure scheme. The lateral boundaries of the model change with time representing the continuous processes of flooding and drying.

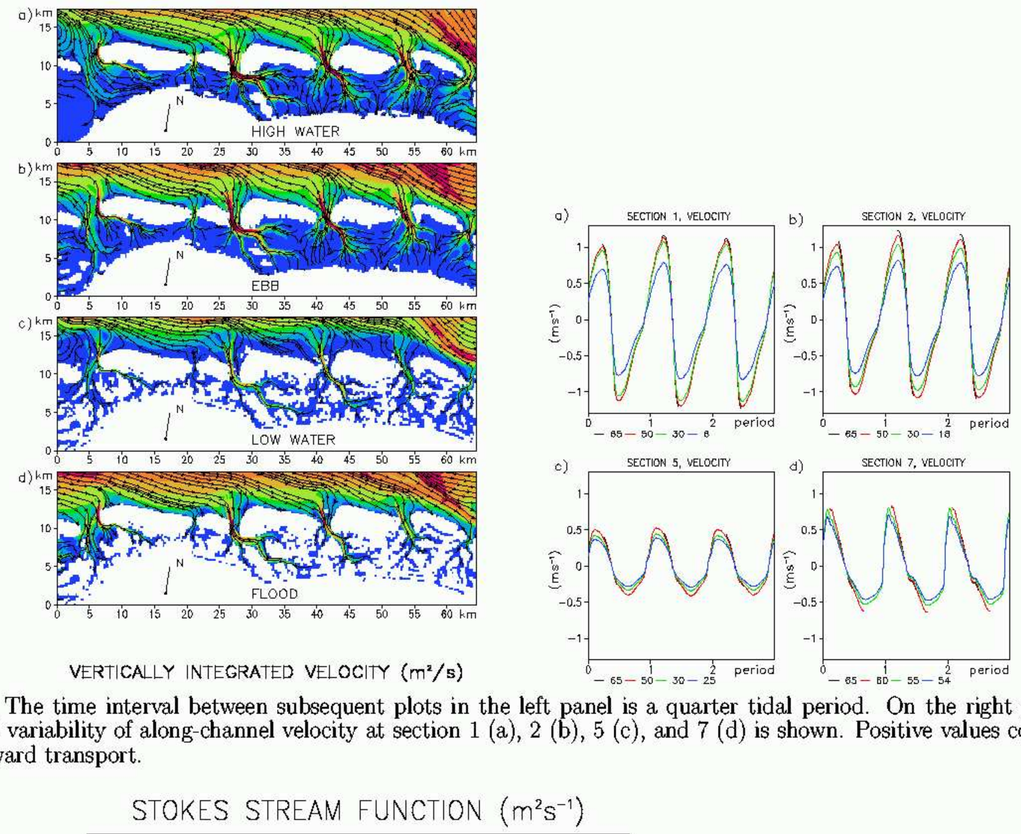

Fig. 8: The time interval between subsequent plots in the left panel is a quarter tidal period. On the right panel the temporal variability of along-channel velocity at section 1 (a), 2 (b), 5 (c), and 7 (d) is shown. Positive values correspond to land ward transport.

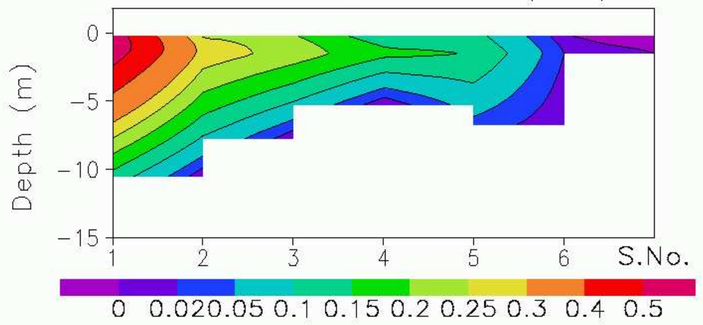

Fig. 9: Stokes stream function illustrating the landward transport in the surface layer and the seaward transport in the deep layer.

Acknowledgments: We are indebted to B. Flemming for providing the ADCP data.

References

[1] Burchard H, Bolding K (2002) GETM - a general estuarine transport model. Scientific Documentation, No EUR 20253 EN, European Commission, printed in Italy, 157 pp

[2] Dyer K (1988) Fine sediment particle transport in estuaries. In: Dronkers J, van Leusem W (eds) Physical processes in estuaries, Springer-Verlag Berlin Heidelberg, Germany, 298-310

[3] Maas LRM (1997) On the nonlinear Helmholtz response of almost enclosed tidal basins with sloping bottoms. J Fluid Mech 349: 361-380

[4] O'Brien MP (1936) The lag and reduction in range in tide gage wells. Technical Memo No 18, US Tidal Model Laboratory, Berkeley CA.

[5] Stanev EV, Flöser G, Wolff J-O, (2003b), Dynamical control on water exchanges between tidal basins and the open ocean. A Case Study for the East Frisian Wadden Sea, Ocean Dynamics, PECS 2002 Special Issue, (in press).

[6] Stanev EV, Wolff J-O, Burchard H, Bolding K, Flöser G, (2003a), On the Circulation in the East Frisian Wadden Sea: Numerical modelling and data analysis, Ocean Dynamics, Vol 53(1), 27-51